

Fabrication of Highly-Aligned, Conductive and Strong Graphene Papers Using Ultralarge Graphene Oxide Sheets – Supporting Information

*¹Xiuyi Lin, ¹Xi Shen, ¹Qingbin Zheng, ¹Nariman Yousefi, ²Lin Ye, ²Yiu-Wing Mai and ¹Jang-Kyo Kim**

¹Department of Mechanical Engineering, The Hong Kong University of Science and Technology, Clear Water Bay, Kowloon, Hong Kong

²Centre for Advanced Materials Technology, School of Aerospace, Mechanical and Mechatronic Engineering, The University of Sydney, Sydney, NSW 2006, Australia

*To whom correspondence should be addressed: mejkkim@ust.hk

S1. Materials, preparation of GO dispersion and GO papers

The precursor GO was synthesized based on the modified chemical method^{1,2} using expanded graphite. Natural graphite flakes (Asbury Graphite Mills) and sulfuric acid (H₂SO₄, 95.5-96.5%, General Chemical) were mixed and then nitric acid (HNO₃, 69–72% Fisher) was added into the mixture. After magnetic stirring for 24 h, de-ionized (DI) water was poured slowly into the mixture. The resultant mixture was washed using DI water three times, which was then dried at 60°C overnight to obtain graphite intercalation compound (GIC). The dry GIC powder was expanded at 1050 °C for 15 sec in a tube oven to obtain expanded graphite (EG). Sulfuric acid and KMnO₄ were added to EG, followed by stirring for 24 h. The solution was transferred to an ice bath, and DI water and H₂O₂ were poured slowly into the mixture where the color of the suspension changed from dark green to light brown. Having stirred for another 30 min, graphene

oxide (GO) was obtained, which was washed with HCl solution and DI water until the pH of the solution became about 5 to 6. The obtained GO particles were diluted with DI water (~1.0 mg/ml) and sonicated for 20 min using a bath sonicator.

GO sheets were examined on a scanning electron microscope (SEM) and an atomic force microscope (AFM), as shown in Figure S1. The as-prepared GO before centrifugation had a lateral dimension ranging from less than 1 to more than 40 micrometers. The AFM image shows a flat GO sheet with a height around 1.105 nm, indicating a monolayer GO.¹

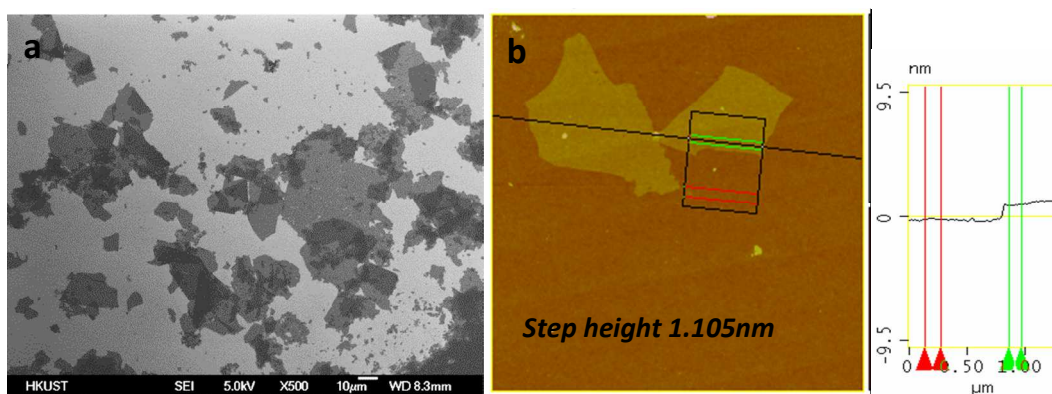


Figure S1 – (a) Typical SEM image of GO, (b) AFM image (5 μm x 4 μm scan) of monolayer GO of thickness 1.105 nm.

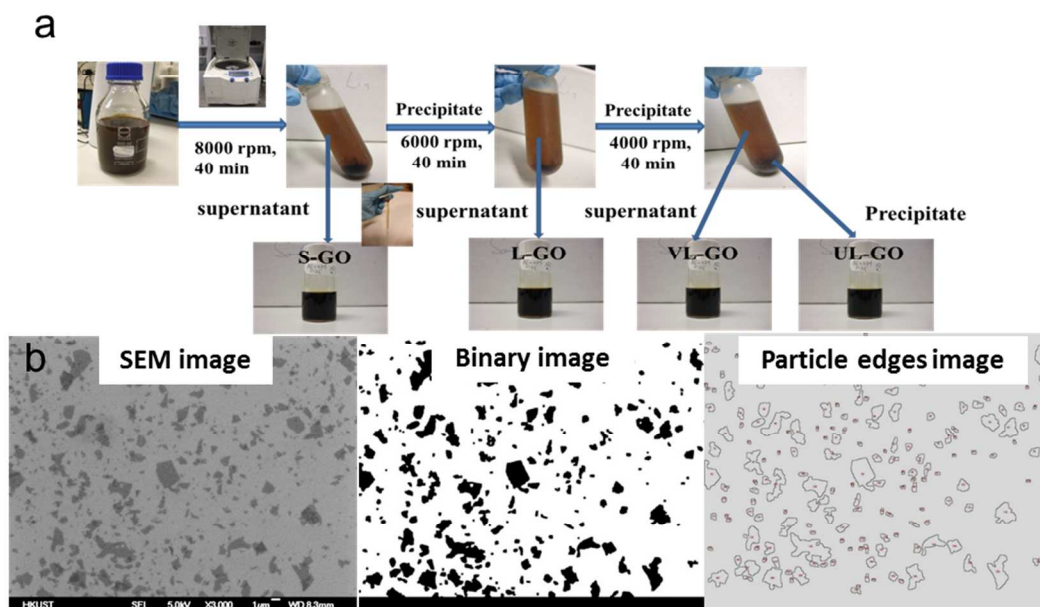


Figure S2. (a) Flowchart for GO sorting process by 3-step centrifugation; (b) GO sheet size analysis using ImageJ.

Four different size groups of GO were sorted through three-step centrifugation of as-prepared GO (Figure S2a), and their average areas and perimeters were measured using the software, ImageJ (Figure S2b).

Three different methods were used to reduce the GO or GO papers at different stages of fabrication, as shown in Figure S3. They included (i) reduction of GO sheets using hydrazine, (ii) reduction of GO papers by immersing in hydrogen iodine (HI) solution and (iii) reduction of GO papers through high temperature treatment. Further details of these processes are described below.

Hydrazine reduction. The GO suspension was mixed with hydrazine (N_2H_2 in water, 35%, Aldrich) and ammonia mixture ($\text{NH}_3\cdot\text{H}_2\text{O}$, 28–30 wt.%, Wako) in the weight ratio of hydrazine/ammonia to GO \approx 7:10 to produce a stable dispersion of highly conducting reduced GO (rGO) sheets.² After stirring for a few minutes, the mixture was placed in a warm oil bath for 1 hr. To avoid aggregation of rGO after reduction, $\text{NH}_3\cdot\text{H}_2\text{O}$ was used to adjust the pH in the range of 10–11 and the temperature was maintained below 100 °C. The brown dispersion was turned into black after the chemical reduction, which was maintained stable for several days without aggregation.

Hydrogen iodine reduction. The GO papers obtained from vacuum filtration were immersed in hydroiodic acid (HI, 57%, Acros) in a sealed cuvette, and placed the cuvette in a warm oil bath for 1 h. The reduced GO papers were washed by ethanol three times to remove excessive HI.

Thermal reduction. The GO papers were placed inside a ceramic container which was introduced into a high temperature furnace (Thermcraft /Eurotherm) with controlled vacuum and

argon flow. The papers were pre-annealed at a heating rate of 10 °C/min, and held at 400 °C for 1.5 h. After cooling to room temperature, the papers were heated to 1100 °C and held for 30 min.

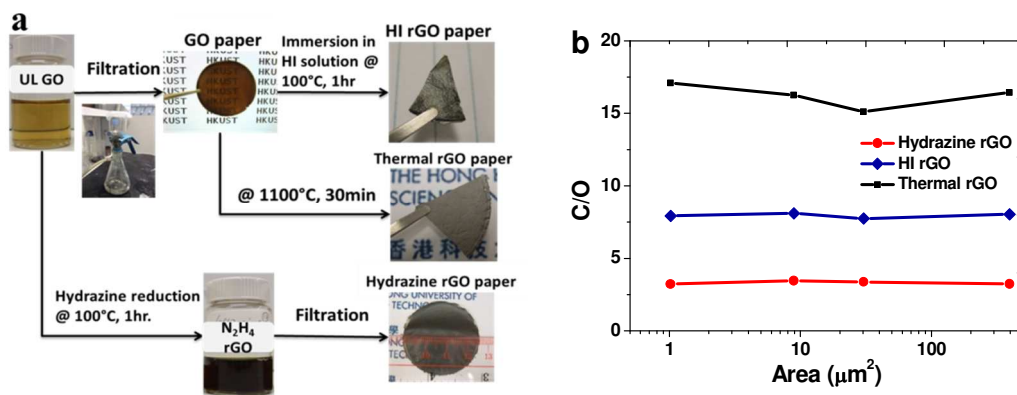


Figure S3. (a) Flowchart for preparation of GO papers and reduction methods to prepare reduced GO papers; and (b) corresponding carbon to oxygen ratios for four different size groups.

Figure S3b indicates that the C/O ratios of GO papers containing four different size groups treated by the same reduction methods were in close proximity with only a marginal difference for thermally reduced GO, indicating that all three reduction processes were not influenced by the GO size. The average values of C/O ratio were 3.5, 7.9, 16.4 for the hydrazine rGO, HI rGO and thermal rGO, respectively.

S2. Characterizations and GO papers

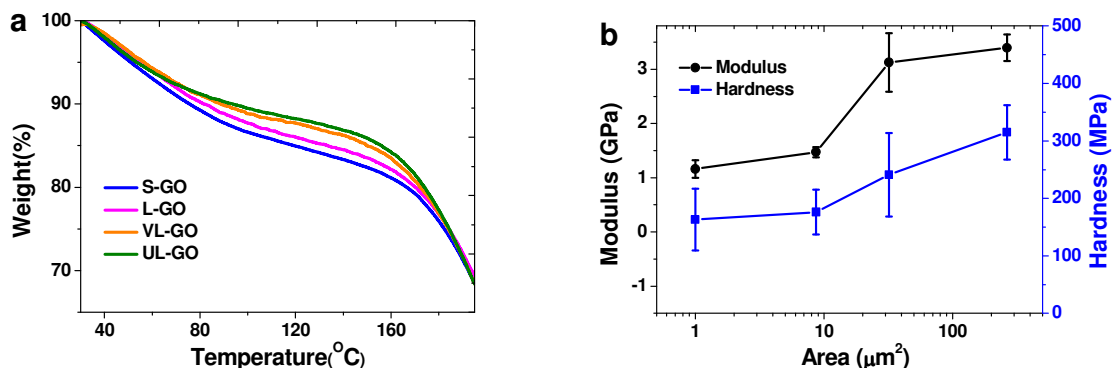


Figure S4. (a) TGA curves for GO papers of four different size groups; (b) changes in nano-indentation properties of GO papers measured as a function of average GO area.

Thermogravimetric analysis (TGA Q500) was performed in an argon gas environment and at a heating rate of 5 °C/min to determine the water contents in the GO papers. Figure S4a presents the TGA curves of GO papers, showing a falling trend with increasing GO size. Nano-indentation tests were conducted to measure the hardness and modulus of GO papers using a 150 nm Berkovich indenter on an ultramicro indentation system (TribolIndenter, Hysitron). There were drastic enhancements in both the modulus and hardness of GO papers with increasing GO size, as shown in Figure S4b. It is also worth mentioning that the modulus measured in tension was 3 to 4 times higher than the corresponding values measured in nano-indentation, for all the GO sizes studied. This is expected in view of the different ways, i.e. in-plane in tensile tests and through-thickness in nano-indentation, that the modulus values were measured. There may also be a negative effect of densification of the porous GO papers under the indentation load.

S3. Statistical analysis of area and perimeter of GO sheets

Based on the two-parameter Weibull model, the cumulative probability, $F(x)$, of GO sheet area or perimeter, x , can be predict by:

$$F(x) = 1 - e^{-\left(\frac{x}{\beta}\right)^\alpha} \quad (1)$$

where α and β are the Weibull modulus and scale parameter, respectively, which can be estimated using the least squares analysis. By taking the natural logarithm of Eq. (1) and rearrangement gives:

$$\ln \left[\ln \left(\frac{1}{1-F(x)} \right) \right] = \alpha \ln x - \alpha \ln \beta \quad (2)$$

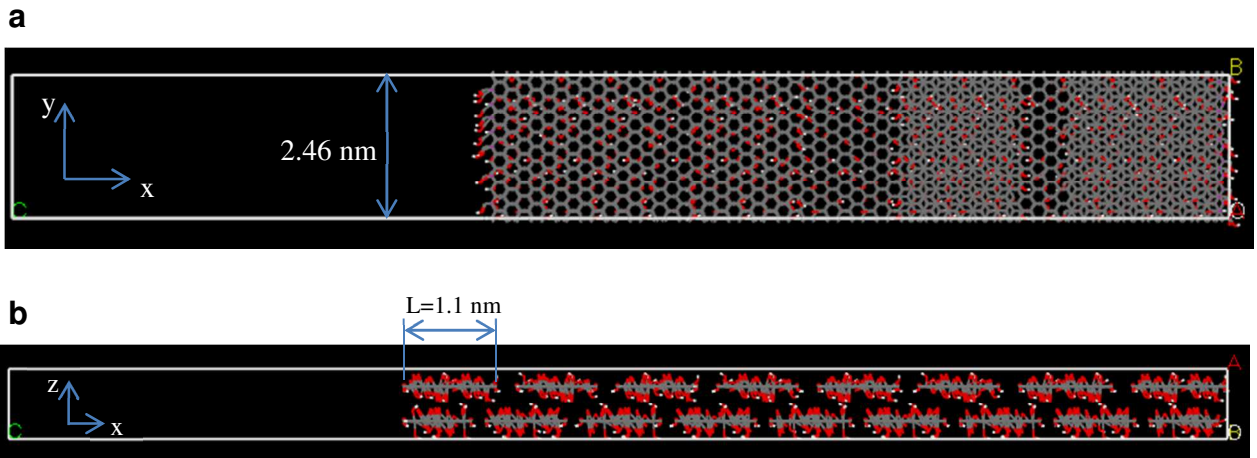
where α can be determined from the regression line, $\ln(x)$ against $\ln\left[\ln\left(\frac{1}{1-F(x)}\right)\right]$. β can be obtained directly from the y-intercept of this line. The cumulative probability of area or perimeter can be estimated by:

$$F(x) = \frac{i}{n+1} \quad (3)$$

$F(x)$ gives the probability of area or parameter under the i th value and n is the total number of GO sheets counted.

S4. Molecular Dynamics Simulation of Graphene Oxide Papers Loaded in Tension

GO paper models. For each set of models with and without water (Figure 6), five different models with the same number of carbon atoms and different GO lengths were constructed where the width and the thickness were kept identical. GO sheets were stacked in a hierarchical manner with individual lengths approximately 1.1 nm, 2.0 nm, 2.4 nm, 3.5 nm and 5.4 nm along the x-axis and a constant width of 2.46 nm in the y-axis. For models without water (Figure 6(a)), an interlayer distance of 6 Å was chosen according to the previous findings^{3, 4}. For models containing water (Figure 6(b)), water molecules were randomly added to the structures, yielding a moisture content of 16 w.t. % and an interlayer distance of 9 Å according to the experimental analysis.



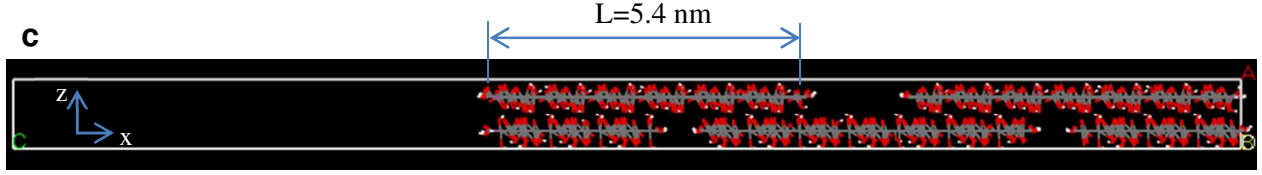


Figure S5. Initial configurations of MDS models of GO paper: (a) x-y plane view where the widths of all models are identical; (b) x-z plane view of the model with GO length of 1.1nm; and (c) 5.4 nm.

Calculation of Young's modulus. The Young's moduli of GO paper models were obtained from the energy-strain curves. The boundary carbon atoms at the right edge were fixed and a displacement ΔL was applied to the carbon atoms at the left edge. The system was then relaxed for 10 ps with a subsequent minimization process to reach equilibrium. The temperature was maintained at 1K to avoid thermal effects because our calculation of Young's modulus was based on the elastic potential energy, which was achieved by energy minimization of the structure at 0 K. The Young's modulus, E , is defined as:

$$E = \frac{\sigma}{\varepsilon} = \frac{F/A}{\Delta L/L_x} = \frac{FL_x}{A\Delta L}, \quad (4)$$

where $A = L_y h$ is the cross-sectional area, and h is the thickness of the model. L_x is the total length of the model along the x-axis. F is the force acting on the carbon atoms along the x-axis, which can be expressed as:

$$F = \frac{EA\Delta L}{L_x}. \quad (5)$$

The strain energy, U , was calculated as:

$$U = \int F dL = \frac{1}{2} E V \varepsilon^2, \quad (6)$$

where $V = AL_x$ is the volume of the model. The Young's modulus is now given by:

$$E = \frac{1}{V} \frac{\partial^2 U}{\partial \varepsilon^2}. \quad (7)$$

Calculation of interaction energy. The interaction potential energy between two adjacent GO sheets can be calculated as:

$$U_{int} = |U_{A,B} - (U_A + U_B)|, \quad (8)$$

where U_A and U_B are the potential energies of two isolated GO sheets, and $U_{A,B}$ is the total potential energy of the assembly.

Extrapolation of Young's modulus to micrometer scale. Due to the limitation of computational capability, the size of simulation models was set on the nano-scale, which was much smaller than the micro-scale of the samples used in experiments. Therefore, the simulation results were extrapolated to predict the Young's modulus of papers with GO sheets on the micro-scale by logarithmic fitting:

$$E = a - b \ln(L + c), \quad (9)$$

where E is the Young's modulus (GPa); L is the length of individual GO sheet (nm); and a , b and c are the coefficients to be fitted by the experimental data.

Calculation of deformation of GO papers. All calculations were conducted based on the same strain level of 0.4%. Supposing ΔL_{total} denotes the total deformation of GO papers, ΔL_{total} is given by the sum of two components: (i) elongation of each GO sheet, $\Delta L_{GO\ sheet}$ and (ii) elongation of the gap between them in the same horizontal plane $\Delta L_{inter-sheet}$:

$$\Delta L_{total} = \Sigma \Delta L_{GO\ sheets} + \Sigma \Delta L_{inter-sheet}. \quad (10)$$

Table S1 Comparison of typical elastic moduli and electrical conductivities of GO and rGO papers measured in this study with those reported in the literature.

GO paper	Young's modulus (GPa)	Tensile Strength (MPa)
UL-GO paper (current study)	13.25	94

Untreated GO paper ⁵	11	66
Untreated GO paper dried at 90 °C ⁶	20	125
Untreated GO paper ⁷	16.6	81.9
Hydrazine reduced GO paper treated at 500 °C ⁸	22	100
Hydrazine reduced GO paper ⁹	21-31	70-78
Reduce graphene oxide-ODA paper ⁹	12-15	31-52
Untreated GO paper ¹⁰	9.1-13	60-70

Reduced GO paper	Conductivity (S/cm)
Thermally reduced UL-GO paper at 1100 °C (current study)	1390
Hydrazine reduced GO ²	72
Hydrazine reduced GO at 150 °C ¹¹	160
GO paper treated at 500 °C ⁸	351
KOH activated reduced GO paper treated at 800 °C ¹²	58.8
Hydrazine reduced GO paper treated at 700 °C under a hydrogen flow ¹³	50
Hydrazine reduced HA modified GO paper treated at 500 °C under vacuum ¹⁴	350

References

1. Zheng, Q. B.; Ip, W. H.; Lin, X. Y.; Yousefi, N.; Yeung, K. K.; Li, Z. G.; Kim, J. K. Transparent Conductive Films Consisting of Ultralarge Graphene Sheets Produced by Langmuir-Blodgett Assembly. *ACS Nano* **2011**, 5, 6039-6051.
2. Li, D.; Müller, M. B.; Gilje, S.; Kaner, R. B.; Wallace, G. G. Processable Aqueous Dispersions of Graphene Nanosheets. *Nat. Nanotechnol.* **2008**, 2, 101-105.

3. Medhekar, N. V.; Ramasubramaniam, A.; Ruoff, R. S.; Shenoy, V. B. Hydrogen Bond Networks in Graphene Oxide Composite Paper: Structure and Mechanical Properties. *ACS Nano* **2010**, *4*, 2300-2306.
4. Compton, O. C.; Cranford, S. W.; Putz, K. W.; An, Z.; Brinson, L. C.; Buehler, M. J.; Nguyen, S. T. Tuning the Mechanical Properties of Graphene Oxide Paper and Its Associated Polymer Nanocomposites by Controlling Cooperative Intersheet Hydrogen Bonding. *ACS Nano* **2012**, *6*, 2008-2019.
5. Stankovich, S.; Dikin, D. A.; Compton, O. C.; Dommett, G. H. B.; Ruoff, R. S.; Nguyen, S. T. Systematic Post-assembly Modification of Graphene Oxide Paper with Primary Alkylamines. *Chem. Mater.* **2010**, *22*, 4153-4157.
6. An, Z.; Compton, O. C.; Putz, K. W.; Brinson, L. C.; Nguyen, S. T. Bio-Inspired Borate Cross-Linking in Ultra-Stiff Graphene Oxide Thin Films. *Adv. Mater.* **2011**, *23*, 3842-3846.
7. Park, S.; Lee, K. S.; Bozoklu, G.; Cai, W.; Nguyen, S. B. T.; Ruoff, R. S. Graphene Oxide Papers Modified by Divalent Ions-Enhancing Mechanical Properties *via* Chemical Cross-Linking. *ACS Nano* **2008**, *2*, 572-578.
8. Chen, H.; Müller, M. B.; Gilmore, K. J.; Wallace, G. G.; Li, D. . Mechanically Strong, Electrically Conductive, and Biocompatible Graphene Paper. *Adv. Mater.* **2008**, *20*, 3557-3561.
9. Ranjbartoreh, A. R.; Wang, B.; Shen, X.; Wang, G. Advanced Mechanical Properties of Graphene Paper. *J. Appl. Phys.* **2011**, *109*.
10. Gao, Y.; Liu, L. Q.; Zu, S. Z.; Peng, K.; Zhou, D.; Han, B. H.; Zhang, Z. The Effect of Interlayer Adhesion on the Mechanical Behaviors of Macroscopic Graphene Oxide Papers. *ACS Nano* **2011**, *5*, 2134-2141.
11. Park, S.; An, J.; Jung, I.; Piner, R. D.; An, S. J.; Li, X.; Velamakanni, A.; Ruoff, R. S. Colloidal Suspensions of Highly Reduced Graphene Oxide in a Wide Variety of Organic Solvents. *Nano Lett.* **2009**, *9*, 1593-1597.
12. Zhang, L. L.; Zhao, X.; Stoller, M. D.; Zhu, Y.; Ji, H.; Murali, S.; Wu, Y.; Perales, S.; Clevenger, B.; Ruoff, R. S. Highly Conductive and Porous Activated Reduced Graphene Oxide Films for High-Power Supercapacitors. *Nano Lett.* **2012**, *12*, 1806-1812.
13. Vallés, C.; David Núñez, J.; Benito, A. M.; Maser, W. K. Flexible Conductive Graphene Paper Obtained by Direct and Gentle Annealing of Graphene Oxide Paper. *Carbon* **2012**, *50*, 835-844.
14. Compton, O. C.; Dikin, D. A.; Putz, K. W.; Brinson, L. C.; Nguyen, S. T. Electrically Conductive “Alkylated” Graphene Paper *via* Chemical Reduction of Amine-Functionalized Graphene Oxide Paper. *Adv. Mater.* **2010**, *22*, 892-896.